Chapter 6

Models of ICM dust

When in section 1.2.4 the question of dust presence in the hot intracluster medium (ICM) of galaxies was raised, a particular emphasis was given on the absence of convincing proofs of its survival in such a hostile medium. The attempts to quantify the amount of dust dispersed in the ICM by using extinction measurements have given contradicting results. The efforts to detect direct thermal emission from such dust have also yielded results which are not fully convincing.

For a better understanding of dust physics in hot plasmas, it is necessary to predict the expected emission, in view of the present and future observational campaigns. This requires a detailed model for the temperature distribution of ICM dust.

An algorithm which derives the temperature of dust embedded in a hot astrophysical plasmas was developed by Dwek (1986). In this chapter a new numerical implementation of this method is discussed, and a parallel code, able to compute the stochastic temperature distribution for a wide range of input parameters, is presented. The case of the Coma clusters of Galaxies is studied, and possible astrophysical applications, are suggested.

This work has been made under the supervision of Dennis W. Sciama at SISSA/ISAS (Trieste, Italy) and in collaboration with Avery Meiksin (now at University of Edinburgh, UK).

6.1 Characteristics of ICM dust

The basic characteristics of ICM dust are described in section 1.2.4. They are inferred from the status of the hot plasma that accumulates at the gravitational well of massive clusters of galaxies, which in turn are mainly derived

by X-ray observations.

The physical status of dust and gas in the ICM is a fundamental ingredient to model the thermal structure of ICM dust, and is reviewed in this section in reference to the specific case of the Coma Cluster of galaxies.

6.1.1 The Coma Cluster of Galaxies

The Coma cluster of galaxies is considered as the archetype of a virialized cluster in state of thermodynamical equilibrium (Kent, 1982). The distance $D \simeq 138$ Mpc, and the high luminosity $L_X \simeq 1.7 \cdot 10^{45}$ erg s^{-1} (Mushotzky et al., 1978) makes the Coma cluster an ideal observational target. It was, in fact, the original cluster in which what has come to be known as dark matter was discovered (Zwicky, 1933).

Even though there are evidences of substructures inside the cluster, its status of disequilibrium is probably not too severe (Briel et al., 1992). The virialization of the galaxies in the cluster allows to derive a smooth law for their distribution, which have been measured by Henriksen & Mushotzky (1986):

$$g(r) = \left[1 + \left(\frac{r}{r_G}\right)^2\right]^{-3/2} \qquad \text{with} \qquad r_G \simeq 0.25 \text{ Mpc} \tag{6.1}$$

The dynamical equilibrium of the cluster is also reflected by the enormous quantities of gas which constitutes the intracluster medium. This gas supports itself in hydrostatic equilibrium against the gravitational field of the cluster, which requires a kinetic temperature of the order of 10^6–10^8 K. The main energy loss at such high temperature is through bremsstrahlung radiation, responsible for the diffuse X-radiation which is the main cooling mechanism for the ICM.

X-ray images of the Coma cluster have been obtained with the ROSAT satellite, and measure its radial brightness distribution. A best fit analytical representation of the azimuthally averaged surface luminosity of the cluster is given by Briel et al. (1992), and corresponds to a modified isothermal King profile (King, 1966):

$$F_X(r) \simeq 3.5 \cdot 10^{-8} \text{ erg cm}^{-2} \text{ sr}^{-1} \left[1 + \left(\frac{r}{r_X}\right)^2\right]^{-1.75} \tag{6.2}$$

where $r_X \simeq 0.42$ Mpc is the core radius of the cluster.

The gravitational binding mass that is inferred for the cluster is $M_{tot} \simeq 1.8 \cdot 10^{15}$ M$_\odot$, assuming a Hubble constant $H_0 \simeq 50$ km s^{-1} Mpc^{-1} (Briel

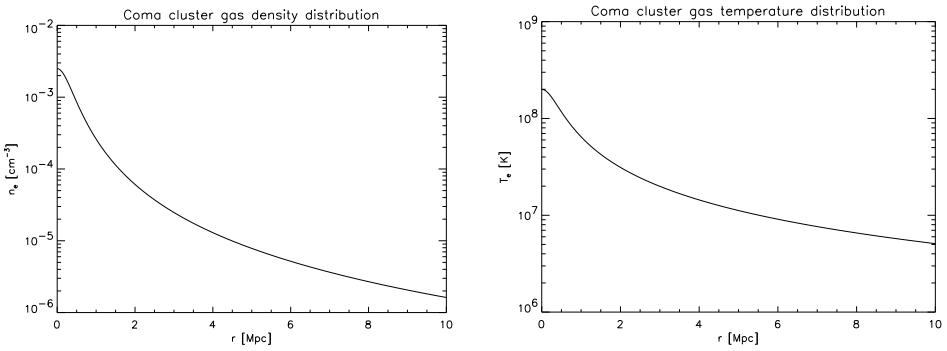

FIG. 6.1.— Radial profiles for ICM gas temperature and density profiles for Coma Cluster. Derived from Henriksen & Mushotzky (1986).

et al., 1992). Since the total mass of the gas ($M_g \simeq 10^{14}$ M$_\odot$) is at least an order of magnitude less (Dwek et al., 1990), one should conclude that most of the gravitational force in the cluster is produced by Dark Matter (DM).

6.1.2 The ICM gas

As for the Coma cluster, the total X-ray luminosity of a rich cluster of galaxies is of the order of 10^{43}–10^{45} L$_\odot$ (Fabian, 1994b). It is from the analysis of this radiation that most of the information on the status of the ICM gas are derived. Emission lines of highly ionized Fe are observed in bright clusters, with ∼0.3 solar abundances. Many other metals are also detected, which equal and even exceed solar abundance (Fabian, 1988). This confirms that the ICM gas is chemically enriched, and cannot be primordial. Its origin is uncertain (see section 1.2.4), but its chemical enrichment suggests its provenience from the galaxies in the clusters.

The spatial density and temperature distribution of ICM gas is also fitted by X-ray surface brightness maps. Best fit profiles for the Coma cluster are plotted in figure 6.1, as given by Henriksen & Mushotzky (1986):

$$n_g(r) \simeq 2.5 \cdot 10^{-3} \text{ cm}^{-3} f(r) \tag{6.3}$$

$$T_g(r) \simeq 2 \cdot 10^8 \text{ K} f(r)^{1/2} \tag{6.4}$$

where

$$f(r) = \left[1 + \left(\frac{r}{r_c}\right)^2\right]^{-1.14} \qquad \text{with} \qquad r_c \simeq 0.4 \text{ Mpc} \tag{6.5}$$

These expressions will be used in section 6.2.4 to compute the temperature distribution of dust at different distances from the center of the cluster.

6.1.3 Size and spatial distribution of the grains

The size and density distribution of dust in the ICM is determined by the time for which the grains have been exposed to the sputtering action of the hot gas. Since typical interstellar grains are smaller than 0.5 μm (see equation 1.1), according to equation 2.70 they cannot survive longer than 10^8 yr in the central region of a rich cluster. Thus, if dust is present in the ICM, it cannot be primordial. As shown in section 1.2.4, injection of dust from the cluster's galaxies is the most plausible hypothesis to explain its presence in the ICM, as inferred by extinction measurements.

Assuming a galactic origin of ICM dust, an initial size distribution similar to MRN distribution (equation 1.1), as for the ISM, is to be expected: $n_d \sim a^{-k}$, with $k = 3.5$. The initial gas to dust mass ratio should also be equal to the galactic value, or $Z_d = 0.0075$.

Once the dust is transferred into the ICM, it is rapidly eroded by the sputtering action of the gas. To guarantee a continuous presence of dust, the injection episodes should occur with a relative frequency (less than 10^8 yr), otherwise the dust disappears. If the dust is continually replenished by the galaxies, a steady state size-diffusion equation can be written (Dwek et al., 1990):

$$\frac{\mathrm{d}n_d(a,r)}{\mathrm{d}a} = \left[\frac{\tau_{sputt}(a,r)}{a}\right]\left[\frac{\mathrm{d}n_{d,i}(a,r)}{\mathrm{d}t}\right] \tag{6.6}$$

where $\mathrm{d}n_d(a,r)$ is the grain number density at distance r and in the size interval a and $a + \mathrm{d}a$, and $\mathrm{d}n_{d,i}(a,r)/\mathrm{d}t$ is the initial injection rate of dust particles of radius a. Assuming all the ICM gas originated in the galaxies, and a constant gas outflow during the lifetime τ_0 of the cluster, then

$$\frac{\mathrm{d}n_{d,i}(a,r)}{\mathrm{d}t} \sim \frac{n_{d,i}(a,r)}{\tau_0} \tag{6.7}$$

where $n_{d,i}(a,r) = n_{d,i}(0) \cdot g(r) \cdot a^{-k}$ is the initial size-density distribution of the injected dust. The dust density at the center of the cluster $n_{d,i}(0)$ is:

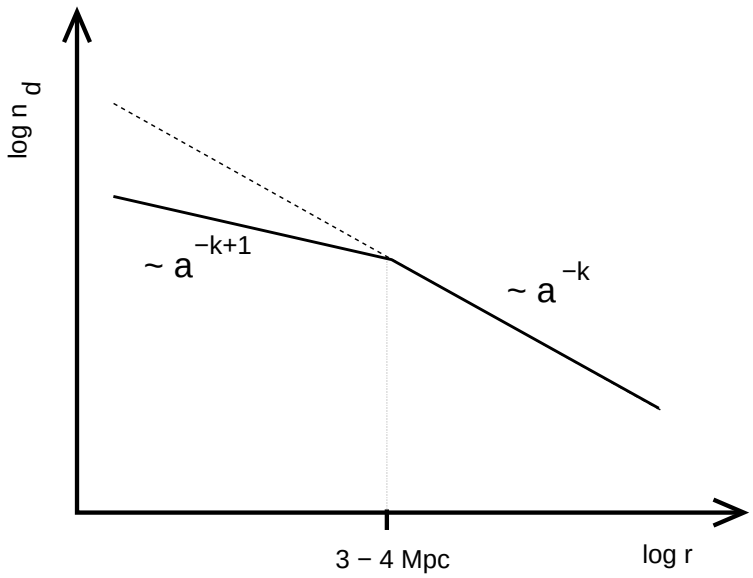

FIG. 6.2.— Schematic profile of Coma cluster dust, with steady state $\sim a^{-k+1}$ radial size distribution in the inner core of the cluster, and ISM like distribution outside the central region, where the dust is not effectively sputtered.

$$n_{d,i}(0) = \frac{\mu_g n_g(0) m_H Z_d}{\langle m_d \rangle} \tag{6.8}$$

where $\mu_g \cdot m_H$ is the mean atomic weight of the gas and $\langle m_d \rangle$ the average mass of the grains in the MNR size interval. From equation 2.70, since $\tau_{sputt} \propto a/n_g$:

$$\tau_{sputt}(a, r) = \frac{\tau_{sputt}(a, 0)}{f(r)} \tag{6.9}$$

Then:

$$\mathrm{d}n_d(a, r) = \frac{\tau_{sputt}(a, 0)}{\tau_0} \cdot \frac{n_{d,i}(0)}{a} \cdot \frac{g(r)}{f(r)} \cdot a^{-k}\, \mathrm{d}a \tag{6.10}$$

The last equation can be integrated with respect to a. Since $\tau_{sputt}/a \sim const(a)$, the only term of equation 6.10 which depends from a is the MRN distribution factor a^{-k}, and then:

$$n_d(a,r) = \frac{\tau_{sputt}(a,r)}{\tau_0} \cdot \frac{\mu_g n_g(0) m_H Z_d}{\langle m_d \rangle} \left[\frac{g(r)}{f(r)}\right] \left(\frac{a^{-k}}{k-1}\right) \tag{6.11}$$

This relation is valid only at distances in which the sputtering time does not exceed the age of the cluster. For the Coma cluster this is true only in the central 3–4 Mpc region, outside of which the dust is not effectively sputtered, and the dust density monotonically increases if continuously ejected by the galaxies (Dwek et al., 1990). The resulting radial profile is shown in figure 6.2.

Equation 6.11 shows that, since $\tau_{sputt} \propto a^{-1}$, steady state ICM dust has a size distribution $n_d(a) \propto a^{-(k+1)}$, which makes it different from the newly injected MNR distribution $n_{d,i}(a) \propto a^{-k}$. A second characteristic of the steady state dust distribution is the radial dependence $g(r)/f(r)$ which reflects the distribution of the dust sources (the galaxies) and destructors (the gas).

6.1.4 Dust properties

Equation 2.77 shows that the cooling rate necessary to derive the thermodynamics of grains, depends on the dust Planck averaged absorption efficiency. This quantity depends on the optical properties of the dust, and thus on its composition and grain size.

Opacities for dust in Active Galactic Nuclei (AGNs) have been derived by Laor & Draine (1993) by applying Mie theory to model grains in the $5 \cdot 10^{-3}$–10 μm size, over the 1000 μm–1 Å range. The optical constants are available for silicates, graphite and SiC, and have been derived by fitting the observed spectra of AGNs from the IR to X.

We have computed the Planck averaged absorption efficiency of silicates and graphite in order to provide the cooling rates of carbonaceous and oxidic dust having different sizes. Our grain size range have been restricted to the $1 \cdot 10^{-3}$–0.1 μm interval, on a grid made of 41 points. For small grains, $Q_\nu(a) \sim a$, and thus Q_P/a is roughly constant. For $\lambda \gtrsim 20$ μm, $Q_\nu \sim \lambda^{-2}$, and thus equation 2.79 gives $Q_P(a,t)/a \propto \lambda^2$. This power-law is valid in our grain size range for low temperatures, where the black body emission is peaked at short wavelength. An example of Planck averaged absorption efficiency for dust grains having $a \simeq 0.01$ μm is given in figure 6.3.

A second ingredient which is used to compute the grain radiative cooling time is their heat capacity (see equation 2.81), which is available as a fit for

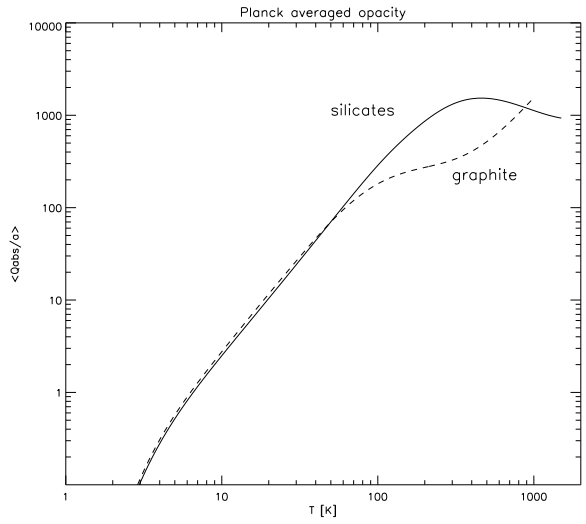

FIG. 6.3.— Planck averaged opacity for Laor & Draine (1993) silicate and graphite grains (the grains size a is in cm).

laboratory data. We have used the power-laws given by Dwek (1986) for graphite grains, and by Draine & Anderson (1985) for silicates.

6.2 Temperature distribution

The thermodynamical status of ICM dust is determined by the balance between radiative cooling and heating. Two heating mechanisms prevails: radiative heating by the background radiation flux in the cluster, and collisional heating due to the electrons of the ICM plasma (see section 2.3.4). If the radiative heating due to the background can be considered continuous, collisional heating depends on the timescales τ_{coll} between two successive grain - electron collisions. If $\tau_{coll} \gtrsim \tau_{cool}$ the grains receive from the gas enough energy to maintain a constant equilibrium temperature, while in the opposite case ($\tau_{coll} \ll \tau_{cool}$) the grains temperature oscillates at each collision.

This section describes our implementation of the model developed by Dwek (1986). First the equilibrium temperature for grains continuously heated is evaluated, and then a method to compute the statistical temperature distribution of stochastically heated grains is explained, and applied to the case of the Coma cluster.

6.2.1 Equilibrium temperature

The equilibrium temperature for collisional heated dust is given by equating the total heating rate provided by the collisions and by the radiation background $H_{coll}(T_d) + H_0(T_0)$, with the radiative cooling rate $\Lambda_{rad}(T_d)$. The background heating rate is in general given by two components: a low energy background caused by the Cosmic Microwave Background Radiation (CMBR), and a high energy flux due to the cluster X-ray emission:

$$H_0 = F_X + 4\pi a^2 \, Q_P(T_{CMBR}) \, \sigma T_{CMBR}^4 \tag{6.12}$$

The collisional heating rate is given by equation 2.73, and depends on the gas parameters (T_e and n_e), the grain size a and the critical energy E_* which regulates the absorption of energy from the colliding electron. For high gas temperatures $E_*/kT_e \gg 1$ the integral in equation 2.73 can be solved with an analytical approximation, giving $H_{coll} \propto a^2 n_g E_*^{3/2}$. Since $E_* \propto a^{2/3}$, then $H_{coll} \propto a^3 n$.

The cooling rate is given by equation 2.77. Using the approximation of the Planck averaged absorption efficiency valid for small grains and low temperatures ($Q_P(a, T_d) \propto a T_d^2$), one has $\Lambda_{rad} \propto a^2 \, T_d^4 \, Q_P(a, T_d) \sim a^3 T_d^6$.

In thermal equilibrium, heating and cooling rate are equal. Neglecting the contribution of the background flux, in this approximation the equilibrium temperature is independent by the grain size and the gas temperature, and is only a function of the gas density. The complete calculation of this result was given by Dwek (1987):

$$T_{eq} \simeq 57\mathrm{K} \, n_g^{1/6} \tag{6.13}$$

with n_g in cm^{-3}, and for $T_e \gtrsim 3 \cdot 10^7$ K. We have tested this relation by solving the equilibrium temperature equation for T_e in the interval 10^6–10^9 K, and $n_e \sim 10^{-6}$–10^{-2} cm^{-3}. The result is shown in figure 6.4. Even though the approximate solution is in the same range of temperature of the exact computation, a certain spread of the equilibrium temperatures is still present, in function of the gas temperature T_e.

Figure 6.4 shows that the equilibrium temperature of ICM dust heated by hot ICM gas goes from $\sim T_{CMBR}$ to 40 K. When the X-ray background flux is added, this temperature can be higher, but our calculations show that the main heating factor are the collisions with the gas.

Note that with dust temperatures in this range, the peak of emission would be in the far-IR or millimetric. However,this is not always the case. When the collisions are sporadic and the temperature of the grains is allowed

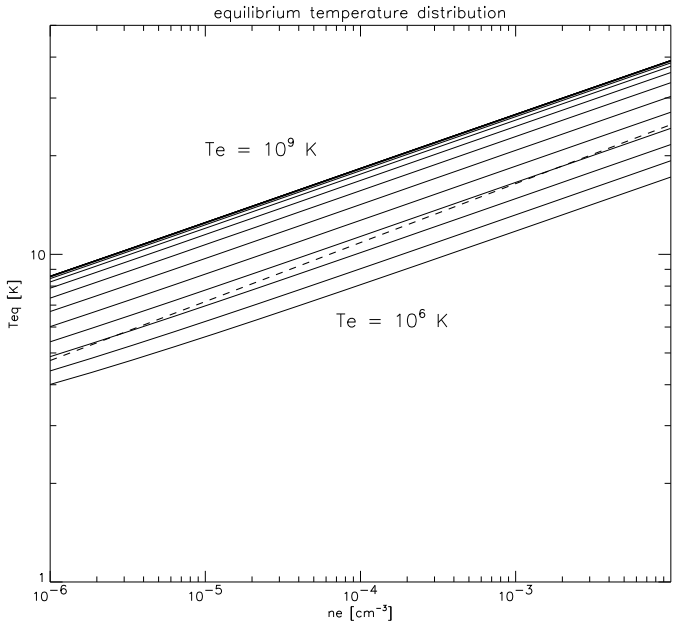

FIG. 6.4.— Equilibrium temperature for ICM dust, computed on a logarithmic grid of electron kinetic temperatures from 10^6 to 10^9 K. The dashed line is the Dwek (1987) approximation in equation 6.13.

to oscillate, a statistical distributions is extablished, as shown in the next section.

6.2.2 Stochastic heating

When the cooling time is much shorter than the interval between collisions of gas particles with the grains, thermodynamical equilibrium cannot be established. In this situation, the idea of "equilibrium temperature" does not make sense anymore, since different grains at different times will not have the same temperature. The only quantity that can be defined in these conditions is a *probability* that a grain of given size a will have temperature T_d when observed.

Assume that, at time t_0, a dust grain of size a is at temperature T_i. Then a collision with a free plasma electron occurs, and a fraction $\zeta(E)$ of the impact energy E is transferred to the lattice of the grain. The final temperature T_f, that is a function of the electron energy and the initial status of the grain, is given by the following equation:

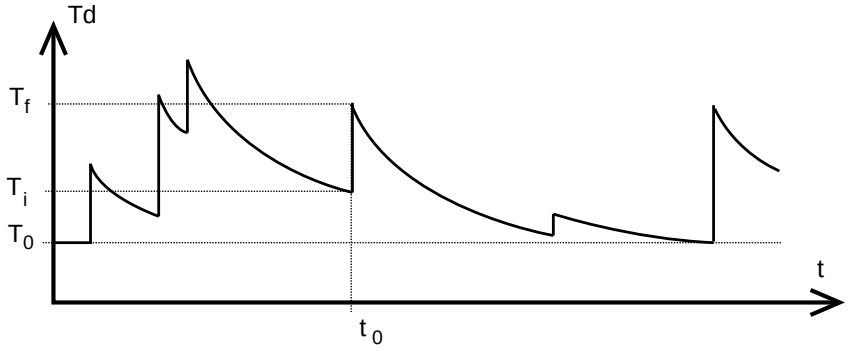

FIG. 6.5.— Temperature oscillations of a stochastically heated dust grain.

$$E\zeta(E) = \int_{T_i}^{T_f} c_V(T)\,\mathrm{d}T \tag{6.14}$$

After the collision, the grain cools down asymptotically toward the minimum temperature T_0 set by the background, until a new scatter raises again its temperature to a different value T_f', according to the energy of the new electron (see figure 6.5).

The rate at which the grain cools down to the minimum temperature T_0 is given by equation 2.80. Since the heat capacity $c_V \propto a^3$ and the Plank averaged absorption efficiency $Q_P \propto a$, this cooling time does not depend on the grain size a:

$$\tau_{cool} \sim \frac{c_V(T_d)}{a^2\,Q_P(a,T_d)} \sim const(a) \tag{6.15}$$

The expected cooling time for silicate and graphite grains ranges from 10^5 s (for $T_f \sim 10$ K) to 10^{-1} s (for $T_f \sim 1000$ K). The expected collision time for ICM with $T_e \sim 10^8$ K and $n \sim 10^{-3}$ cm^{-3} is $\sim 10^3$ s, for grains with $s \sim 5 \cdot 10^{-2}$ μm. Only larger grains (which have a larger cross section and heat capacity) will experience enough collisions to reach thermal equilibrium with the gas. Smaller grains are instead heated to higher T_f (smaller $c_V \propto a^3$), and cool down to lower temperature before another collision (due to their smaller cross sections). These small grains are not in equilibrium with the rest of the ICM.

The fraction of the time spent by a grain cooling down from $T_d + \mathrm{d}T_d$ to T_d with respect to the collision time is given by (Purcell, 1976):

$$P_E(a, T_d)\,\mathrm{d}T_d = \frac{\mathrm{d}t}{\tau_{coll}}\, e^{-\frac{\tau_{cool}}{\tau_{coll}}} \tag{6.16}$$

The probability that a grain of size a is heated to a certain temperature T_d from T_i is obtained by averaging P_E over the flux distribution of the incident electrons:

$$\mathbb{A}_{T_i,T_d} = \langle P_E(a, T_d)\rangle_{nva^2 f(E)} \tag{6.17}$$

For a Maxwellian kinetic temperature distribution of the ICM gas (equation 2.71), the explicit expression of the *transition matrix* $\mathbb{A}(T_d, T_i)$ is:

$$\mathbb{A}_{T_i,T_d} = \theta(T_d) \int_0^\infty e^{-\int_{T_d}^{T_f(x,T_i)} \theta(T)\,\mathrm{d}T} x e^{-x}\,\mathrm{d}x \tag{6.18}$$

where $x = E/kT_e$ and $\theta(T)\mathrm{d}T$ is the *fractional cooling rate*:

$$\theta(T)\mathrm{d}T = \frac{\mathrm{d}T}{\tau_{coll}} \left|\frac{\mathrm{d}T}{\mathrm{d}t}\right|^{-1} \tag{6.19}$$

The transition matrix $\mathbb{A}(T_d, T_i)$ computes the temperature distribution of the grains after one collision, for a grain population of initial temperature T_i:

$$g^{(k)} \equiv G(a, T_d; T_i) \rightarrow g^{(k+1)} = \mathbb{A} g^{(k)} \tag{6.20}$$

After many collisions ($k \rightarrow \infty$), the grain population reaches a "steady state" $g \equiv G(a, T_d)$ in which their temperature distribution does not change after another collision:

$$(1 - \mathbb{A})g = 0 \tag{6.21}$$

This final state is called *stochastic temperature distribution*, and gives the probability $G(a, T_d)\,\mathrm{d}T$ that a grain of size a, in *statistical equilibrium* with the ICM gas, has the temperature T_d.

6.2.3 Numerical approach

An iterative method to compute the "steady state" stochastic distribution $G(a, T_d)$ has been proposed by Dwek (1986). One starts from a stochastic distribution $g^{(0)} = \delta_{T_0,T_i}$ in which grains with all sizes are at the minimum temperature T_0. Then a distribution $g^{(1)}$ is derived by applying the transition matrix to $g^{(0)}$. In other words, this is equivalent to compute the distribution of the grains after one single collision:

$$g^{(1)} = g^{(0)}\,\mathbb{A}_{T_i,T_d} = \delta_{T_0,T_i}\,\mathbb{A}_{T_i,T_d} \tag{6.22}$$

The process is repeated by applying $\mathbb{A}$ to the result of the previous iteration, until convergence is achieved:

$$g^{(k)} = \mathbb{A}\,g^{(k-1)} \rightarrow G(a,T_d) \qquad \text{for } k \rightarrow \infty \tag{6.23}$$

The main computational problem consists mainly in computing the transition matrix $\mathbb{A}$. This requires solving the integral 6.18 for all the combinations of T_i and T_f, ranging from the minimum temperature T_0 to the dust sublimation temperature T_{subl}, and for each grain size a. Since the problem scales as N_T^2, it is necessary to limit the size of the temperature grid, in order to maintain the required computation time at a reasonable level. We used a logarithmic grid for a and T_d, with $N_a = 11$ and $N_{T_d} = 256$.Once the transition matrix is evaluated, one can perform as many iterations as necessary, since the time required for that scales linearly.

The iterations are done only when necessary, i.e. when the collisional time is shorter than the cooling time (the grain does interact with the gas more than once in its lifetime). In the other cases, which are typical of very small grains (with negligible cross sections) only the first iteration is required. For larger grains, a heuristic criteria to determine the number of required iteration is given by:

$$n_{it} \lesssim \frac{\tau_{cool}(T_{eq})}{\tau_{coll}} \tag{6.24}$$

The iterations may be stopped before reaching n_{it}, in case the difference between two successive distribution is less than the allowed precision.

The integrand over x in equation 6.18, should be set to zero when the final temperature T_f is high enough to destroy the grain ($T_F \gtrsim T_{subl}$, see figure 6.6). In this case the grain is removed from the population, and should not contribute to the final statistical distribution. The values of x for which this happens depend on the respective values of the critical energy E_* with the sublimation energy kT_{subl}. To ensure high precision in the integration, without increasing the computation time, the integration is done on an adaptive grid $N_x = 512$ only where the integrand is not zero, and the zero points are computed with a semi-analytic formula.

Since the transition matrix for each set of parameters is evaluated independently, the problem is easily parallelizable, and ideally scales with the number of CPUs that are employed. We have thus written a parallel version of the program, running either using the parallel library MPI (Message

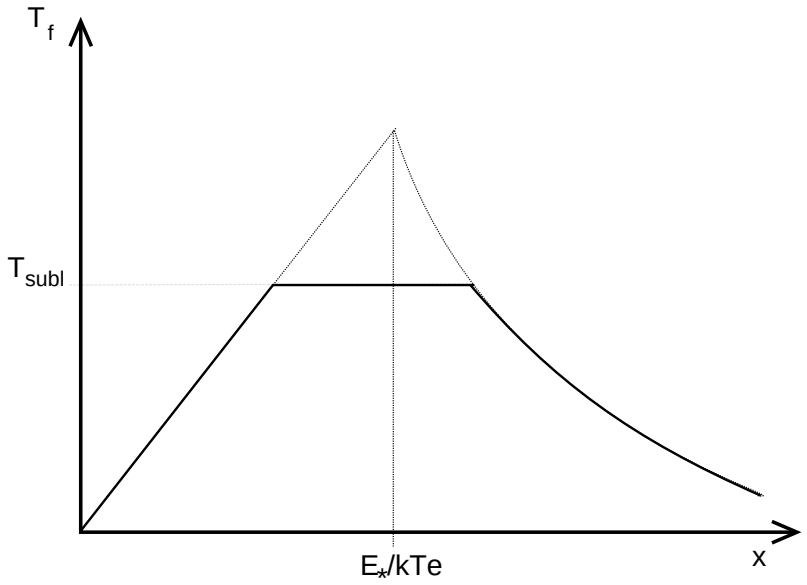

FIG. 6.6.— Final grain temperature as a function of incident electron energy. For $x = E_*/kT_e \gtrsim T_{subl}$ the grain is destroyed, and its contribution to the statistical equilibrium of temperatures should be removed.

Passing Interface, Gropp et al. 1999) or PVM (Parallel Virtual Machine, Geist et al. 1994). The code is able to compute a full grid of 15 T_e,n_e pairs (e.g. the status of the the ICM gas in 15 radial annuli from the center of a cluster) in about 6 hours, with the SISSA SP2 cluster using 15 nodes.

6.2.4 Modeling results

As a benchmark test for the numerical code, we have computed the stochastic temperature distributions for silicate and graphite dust in the case of the Coma cluster. The radial size-density distribution was evaluated by using equation 6.11, and the ICM gas temperature and density profiles with equations 6.4 and 6.3. The X-ray background flux was estimated by using equation 6.2. The distributions $G(a, T_d)$ have been computed on a logarithmic radial grid of 15 points, from the center of the cluster, to 5 Mpc.

The equilibrium temperatures of the grains are given in table 6.1, for different distances from the center of the cluster, and for different grain-sizes. Note that T_{eq} is largely independent from a, as found by Dwek (1987).

A selection of the dust stochastic temperature distributions is shown in figure 6.7 for silicates, and 6.8 for graphite.

Table 6.1 Dust equilibrium temperature for Coma cluster.

Radius	T_{eq} [K] silicate dust			T_{eq} [K] graphite dust		
(Mpc)	0.001 μm	0.01 μm	0.01 μm	0.001 μm	0.01 μm	0.01 μm
0.00	29.3	30.2	30.2	30.6	30.7	30.7
0.20	28.0	30.0	30.0	29.4	29.4	29.4
0.26	27.3	28.3	28.3	28.7	28.8	28.8
0.33	26.4	27.4	27.4	27.8	27.8	27.8
0.42	25.3	26.2	26.2	26.7	26.7	26.6
0.54	23.9	24.8	24.8	25.2	25.3	25.2
0.69	22.3	23.3	23.1	23.7	23.7	23.5
0.88	20.7	21.6	21.4	22.0	22.0	21.8
1.13	19.0	19.2	19.6	20.3	20.3	19.9
1.45	17.4	18.2	17.7	18.7	18.7	18.1
1.86	15.9	16.7	15.9	17.1	17.1	16.2
2.38	14.5	15.2	14.2	15.6	15.6	14.4
3.05	13.3	13.8	12.5	14.3	14.2	12.7
3.90	12.1	12.5	10.9	13.0	12.8	11.0
5.00	11.0	11.3	9.3	11.8	11.6	9.5

Note the flat shape of the small grain distributions, which are peaked at a temperature close to T_0, but have a long tail reaching high temperatures, up to T_{subl}. This high temperature tail is responsible to a broadening of the emission spectra, which is important due to the dominance of the size distribution towards small grains.

Large grains, as expected, tend instead to the equilibrium temperature. The larger the grain radius, and the more the temperature distribution resembles a δ-function peaked to the equilibrium temperature T_{eq}:

$$G(a, T_d) = \begin{cases} \delta(T_d - T_0) & \text{for } a \to 0 \\ \delta(T_d - T_{eq}) & \text{for } a \to \infty \end{cases} \tag{6.25}$$

Note also the dependence of the $G(a, T_d)$ shape on the dust gas temperature and density: in the more external regions of the cluster, where the gas is colder and more rarefied, even large dust grains cannot experience enough collisions to approach the equilibrium temperature, resulting in broader temperature distributions.

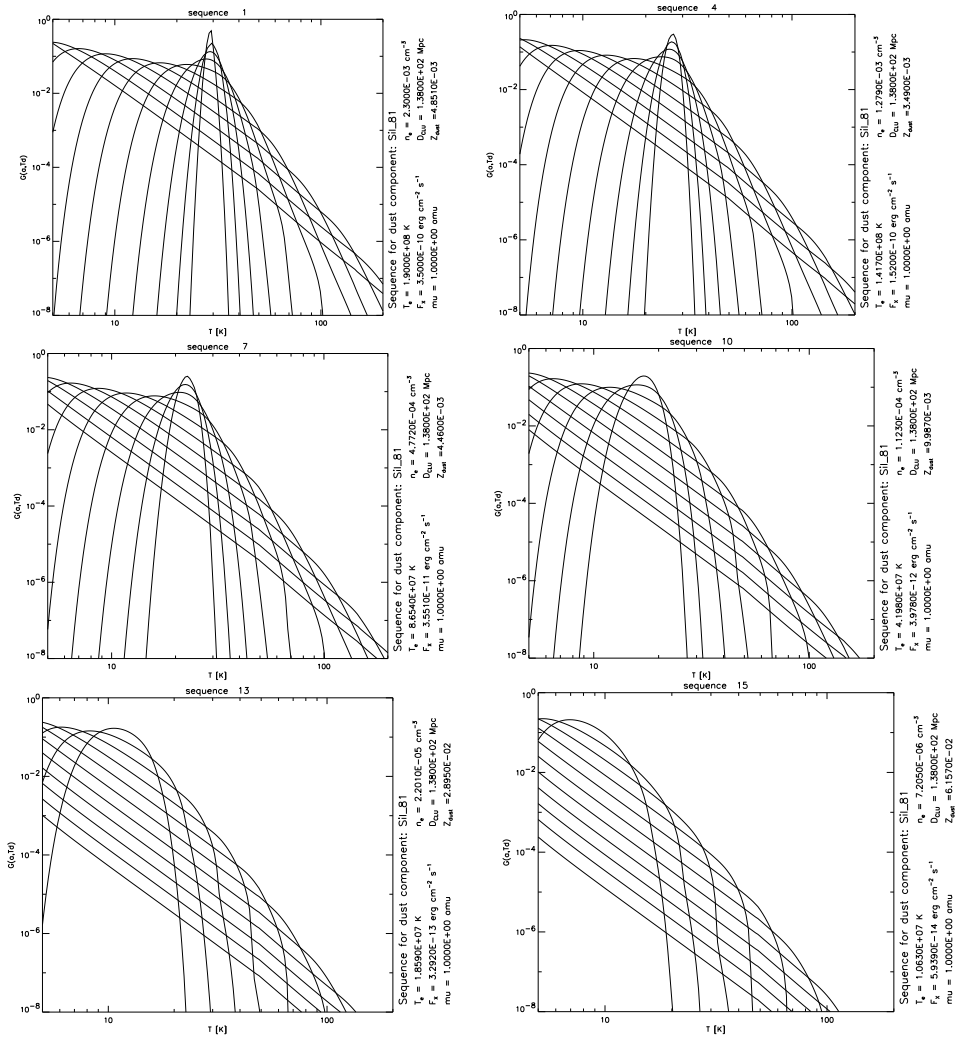

FIG. 6.7.— Stochastic temperature distribution for silicate grains, computed for various annuli from the center of the Coma cluster. Each curve corresponds to a particular grain size, from $a \simeq 0.001$ μm (flat distribution) to 0.1 μm (peaked distribution). The ICM parameters are written on the side of each panel.

As a test we tried to run the same sequence without the X-ray background flux, finding that the contribution of the X-ray to the temperature distribution is of the order of 1 K in the minimum temperature T_0. This confirms that the energy balance of the ICM dust is dominated by the collisions with the hot gas.

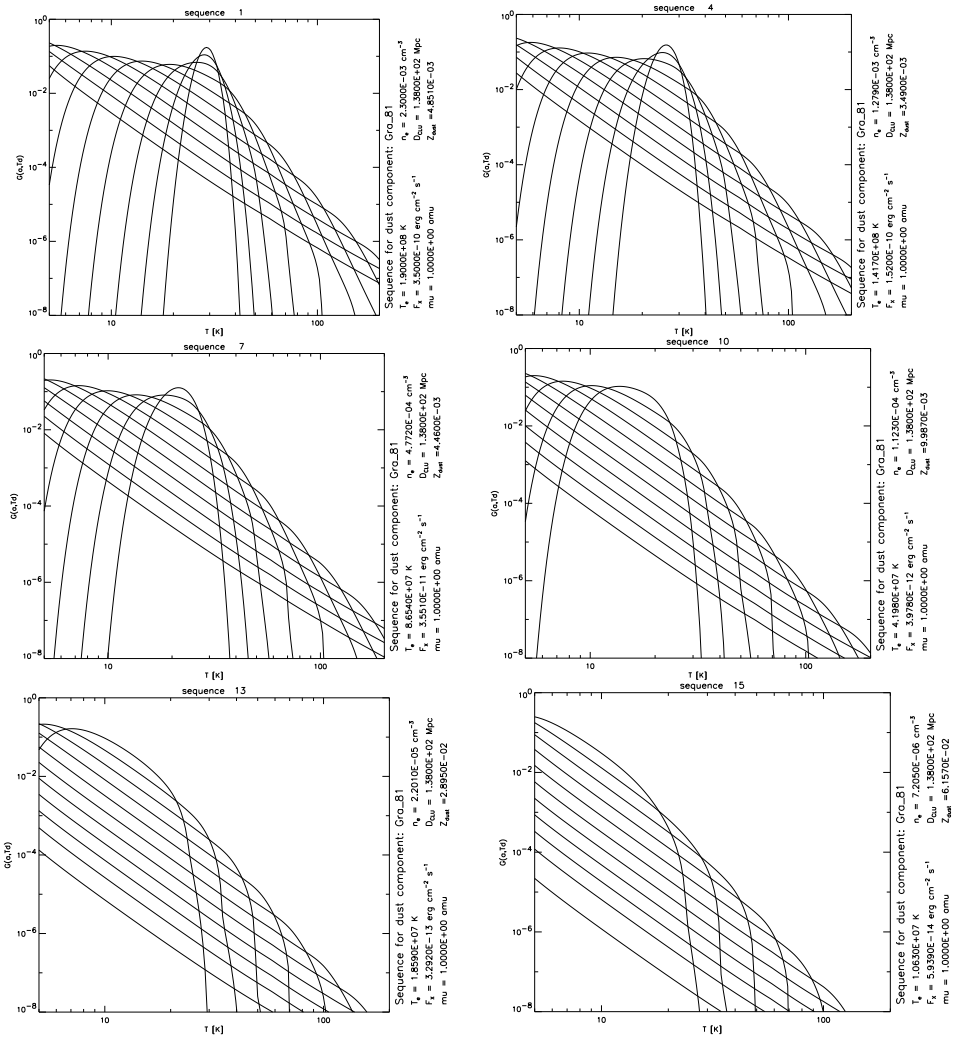

FIG. 6.8.— Stochastic temperature distribution for graphite grains, computed for various annuli from the center of the Coma cluster. Each curve corresponds to a particular grain size, from $a \simeq 0.001$ μm (flat distribution) to 0.1 μm (peaked distribution). The ICM parameters are written on the side of each panel.

6.3 Possible applications

The numerical code here developed is able to compute with excellent accuracy and efficiently the stochastic temperature distribution of dust in hot plasma, subjected by a background radiation field. The most direct application of the code is to compute the spectrum and IR - millimetric surface

brightness of a real cluster, given a map of the temperature and density of the gas, with arbitrary geometry.

In spherical geometry the intensity of the dust radiation can be calculated by extending equation 2.31 to the stochastic temperature case. In optically thin conditions:

$$I_\nu(y) = \int \mathrm{d}\ell \int \mathrm{d}a\, \pi a^2\, Q_\nu(a)\, n_d(a,\ell)\, \langle B_\nu(T_d)\rangle \tag{6.26}$$

where the Planck emissivity is substituted with its average on the statistical distribution $G(a, T_d)$:

$$\langle B_\nu(T_d)\rangle = \int_0^\infty G(a,T_d)\, B_\nu(T_d)\, \mathrm{d}T_d \tag{6.27}$$

Note that in equation 6.26 $Q\nu(a) \sim a$, $n_d(a,\ell) \sim a^{1-k}$ for steady state dust injection from the galaxies, and $n_d(a,\ell) \sim a^{-k}$ for unique episode of sudden injection. In the two cases the emissivity is:

$$I_\nu \propto \begin{cases} a^{4-k} \sim a^{1/2} & \text{for steady state dust injection} \\ a^{3-k} \sim a^{-1/2} & \text{for sudden injection} \end{cases} \tag{6.28}$$

This result shows that from the IR - millimetric spectra of ICM dust it is possible to infer the origin of the dust, and test the interactions between the ISM of the cluster's galaxies, and the ICM. For the Coma cluster the expected flux is of the order of 10^{-1} mJy at 10 μm and 10^3 mJy at 100 μm, which is above the expected sensitivity of the SIRTF photometers.

Another interesting application is to test the effect which dust emission has on the Sunyaev-Zel'dovich (SZ) effect (Sunyaev & Zel'dovich, 1972). The SZ effect is a consequence of Compton scattering of CMBR photons by the hot ICM gas, which results in a characteristic spectral signature. As a consequence of the comptonization of the CMBR, the cluster becomes a "positive" radiation source in the sub-millimeter band, and a "negative" one at larger wavelengths.

This effect is of cosmological interest because it serves as a probe of intracluster gas and its evolution and, when combined with X-ray observations, can be used to estimate the Hubble constant, independent of the distance ladder (Birkinshaw & Hughes, 1994). The SZ effect has been measured in numerous clusters of galaxies, and in particular in the Coma cluster (Herbig et al., 1995; Silverberg et al., 1997).

The measurement of the SZ effect at radio frequencies is complicated by the presence of weak background sources, which may lead to significant

systematic errors of either sign. At millimetric wavelengths, high quality ground-based measurements have been obtained using different techniques with an array of detectors (Wilbanks et al., 1994), or with balloon-borne instruments (Cheng et al., 1994). Given the temperature distribution of ICM dust a certain contribution to the effect from the dust should be expected at millimetric wavelengths.

This contribution can be evaluated as follows. The comptonization parameter of the radiation along the line of sight is a function of the gas density and temperature:

$$y = \left(\frac{k\sigma_T}{mc^2}\right) \int n_e \, T_e \, \mathrm{d}\ell \tag{6.29}$$

The difference in the CMBR intensity at a frequency ν, along different line of sight ℓ, then is (Rephaeli, 1995):

$$\Delta I = \frac{2\left(kT_{CMBR}\right)^3}{\left(hc\right)^2} g(x) \Delta y \tag{6.30}$$

where $x = h\nu / kT_{CMBR}$ and

$$g(x) = \frac{x^4 e^x}{\left(e^x - 1\right)^2} \left[x \coth\left(\frac{x}{2}\right) - 4 \right] \tag{6.31}$$

By using the equations 6.3 and 6.4 it is is possible to compute ΔI, and then compare its spectrum with the spectrum of the expected dust emissions for different dust to gas mass ratios. Alternatively, the millimetric measurements of the SZ effect can be used to derive an estimate (or an upper limit) of the dust density in the cluster, providing an independent test for the survival of dust in the ICM.